Neuron, Vol. 30, 51–64, April, 2001, Copyright ©2001 by Cell Press

Epileptic Seizures May Begin Hours in Advance of Clinical Onset: A Report of Five Patients

Clinical Study

Brian Litt,[1,7] Rosana Esteller,[2,6] Javier Echauz,[2,3] Maryann D'Alessandro,[2] Rachel Shor,[2] Thomas Henry,[5] Page Pennell,[5] Charles Epstein,[5] Roy Bakay,[4,8] Marc Dichter,[1] and George Vachtsevanos[2]

[1]Department of Neurology and Bioengineering
3 West Gates
Hospital of the University of Pennsylvania
3400 Spruce Street
Philadelphia, Pennsylvania 19104
[2]Georgia Institute of Technology
School of Electrical and Computer Engineering
777 Atlantic Drive
Atlanta, Georgia 30332
[3]Electrical and Computer Engineering Department
University of Puerto Rico
Mayagüez, Puerto Rico 00681
[4]Department of Neurosurgery
[5]Department of Neurology
Emory University School of Medicine
1365 Clifton Road, NE
Atlanta, Georgia 30322
[6]Dpto. Tecnología Industrial
Universidad Simón Bolívar
Caracas, Edo. Miranda
Venezuela Aptdo. Postal 89000

Summary

Mechanisms underlying seizure generation are traditionally thought to act over seconds to minutes before clinical seizure onset. We analyzed continuous 3- to 14-day intracranial EEG recordings from five patients with mesial temporal lobe epilepsy obtained during evaluation for epilepsy surgery. We found localized quantitative EEG changes identifying prolonged bursts of complex epileptiform discharges that became more prevalent 7 hr before seizures and highly localized subclinical seizure-like activity that became more frequent 2 hr prior to seizure onset. Accumulated energy increased in the 50 min before seizure onset, compared to baseline. These observations, from a small number of patients, suggest that epileptic seizures may begin as a cascade of electrophysiological events that evolve over hours and that quantitative measures of preseizure electrical activity could possibly be used to predict seizures far in advance of clinical onset.

Introduction

Epilepsy affects 50 million people worldwide, 25% of whom have seizures that cannot be controlled by any available therapy. In most cases, this is *focal* epilepsy, in which seizures arise from a region of abnormal brain, the epileptic focus, and spread in a stereotyped, individualized fashion. 50 years ago, Penfield and colleagues found localized abnormal discharges on the EEG prior to clinical seizures in some affected individuals (Penfield and Erickson, 1941). They reported that seizures could be cured in these patients by removing the brain region that gave rise to this activity (Penfield and Flanigin, 1950; Feindel et al., 1952). Since that time, recognizing seizure onset on EEG has remained the gold standard for locating epileptic foci in the brain (Sperling, 1986).

One of the most disabling aspects of epilepsy is that seizures appear to be unpredictable. Investigation to elucidate their underlying mechanisms has traditionally focused on seconds to minutes before clinical seizure onset. Ralston and Dichter reported preseizure EEG changes consisting of increased frequency and complexity of epileptiform discharges, commonly called spikes, which became polyphasic (developed multiple peaks), rhythmic, and sustained as seizures approached (Ralston, 1958; Dichter and Spencer, 1969a, 1969b). They postulated mechanisms initiating rapid changes in neuronal function, effected by ion channels, neurotransmitters, and the cell membrane. Despite over 40 years of investigation into the physiology of epilepsy, it is still not possible to explain how and over what time spontaneous clinical seizures emerge from the relatively normal brain state observed between them.

In recent years, clinical epilepsy monitoring has enabled studying human seizures quantitatively, as they develop in vivo. This effort has been aided by technological advances such as digital video-EEG monitoring systems that can process data in real time, and safe, reliable electrodes for implantation directly on or in the brain (intracranial electrodes). Most work in quantitative analysis of human seizures has focused on *detecting* their electrical onset on EEG in the up to 10 s that may precede their first clinical signs (clinical onset) (Gotman, 1987, 1991; Qu and Gotman, 1997; Osorio et al., 1998). As early as 1970, researchers considered methods for predicting epileptic seizures prior to electrical onset, though none were implemented clinically (Viglione et al., 1970; Rogowski et al., 1981). Recent research in seizure prediction uses the theory of chaotic dynamics to track nonlinear parameters, such as the principal Lyapunov exponent and correlation dimension, over minutes prior to EEG onset of temporal lobe seizures (Iasemidis et al., 1990, 1994; Lehnertz and Elger, 1998; Martinerie et al., 1998; Le Van Quyen et al., 2001). These studies are important because most support the idea that seizures develop over time, rather than occur as abrupt, isolated events. They are somewhat limited, however, because most concentrate on relatively few or brief data segments prior to seizures, and the abstract parameters they explore are difficult to relate to the neurophysiology of epilepsy.

Because many patients report nonspecific, stereotyped symptoms hours in advance of seizures (Rajna et al., 1997), we have focused on looking for quantifiable

[7]To whom correspondence should be addressed (e-mail: littb@mail.med.upenn.edu).
[8]Present Address: Chicago Institute of Neurosurgery and Neuroresearch, Department of Neurosurgery, Rush-Presbyterian-St. Luke's Medical Center, 1653 West Congress Parkway, Jelke, Suite 1491, Chicago, Illinois 60612.

Table 1. Patient Characteristics

Pt	Sz Types	MRI	FDG Activity	Ictal Onset Zone(s) on Intracranial EEG and Comments	Side of Temporal Resection and Outcome	Seizure Risk Factors
1*	SP	Left hippocampal atrophy	Left temporal decrease	Left hippocampus (6/6)	Left	CHI
	CP			Incomplete resection due to language localization in ictal onset zone	Class II	FS
2	SP	Normal	Equal bilateral temporal decrease	Left hippocampus (11/13)	No surgery	None
	CP			Right hippocampus (2/13) Accumulated energy lateralized to side of onset in all seizures; all Sz propagated in < 3 s to contralateral side		
3	SP	Right frontal venous angioma	Bilateral temporal decrease	Right hippocampus (9/11)	Right	None
	CP			Left hippocampus (2/11) Accumulated energy lateralized to the right in all seizures	Class I	
4	SP	Normal	Right temporal decrease	Right hippocampus (5/5)	Right	None
	CP GTC				Class II	
5	CP	Subependymal heterotopia adjacent to left lateral ventricle	Left temporal decrease	Left hippocampus (6/10)	Left	FS
				Left temporal neocortex (3/10) Right frontal neocortex (1/10) Accumulated energy lateralized to side of onset in all seizures	Class III	

Class of outcomes refers to "Engel Classification" (Engel, 1987): Class I, free of disabling seizures; Class II, rare disabling seizures; Class III, worthwhile improvement; Class IV, no worthwhile improvement.
* Earliest EEG changes associated with seizures were localized to one or two adjacent electrode contacts.
Abbreviations: CP, complex partial; GTC, generalized tonic-clonic; SP, simple partial; CHI, closed head injury with loss of consciousness and/or amnesia; FS, febrile seizures in early childhood.

precursors of seizures far in advance of seizure onset on the EEG. We analyzed continuous intracranial EEG recordings over many days and used algorithms that are sensitive to the spikes, high-frequency rhythmic discharges, and high-amplitude slow waves that are typical of the EEG in epilepsy. This preliminary investigation in five patients is a necessary first step in identifying quantitative parameters worthy of more intensive study in a larger, prospective trial.

We chose to study patients with mesial temporal lobe epilepsy, in whom seizures arose from the amygdala, hippocampus, or adjacent cortex in one or both temporal lobes because: (1) mesial temporal lobe epilepsy frequently cannot be controlled by antiepileptic drugs, (2) it is common and is among the best understood of focal epilepsies, (3) it is common practice to record from intracranial electrodes in these patients during evaluation for epilepsy surgery, (4) the likelihood of electrodes being placed in or very close to the region generating the earliest precursors of seizures is high in these cases, and (5) electrical seizure onsets are usually well localized on intracranial EEG in mesial temporal lobe epilepsy, have high signal to noise ratio, and offer the best available data for studying seizure generation in humans.

Clinical Background

We analyzed data from five patients with mesial temporal lobe epilepsy who required monitoring with intracranial electrodes during evaluation for epilepsy surgery. Subjects were the first five patients meeting these criteria admitted to the Epilepsy Monitoring Unit after university approval of the research protocol. Patients included four men and one woman. Mean age was 32 years (range 21–50). The etiology of epilepsy was likely closed head injury in patient #1, although she also had febrile convulsions in early childhood, which have been associated with later development of mesial temporal lobe epilepsy. Patient #5 also had febrile convulsions, but no other risk factors for epilepsy. The other three patients had no identified risk factors.

Intracranial monitoring was required in these patients because brain imaging, scalp EEG, and other noninvasive studies did not definitively identify the site(s) from which seizures originated. Evaluations included: (1) recording seizures with scalp EEG electrodes, (2) high-resolution brain magnetic resonance imaging (MRI) to look for focal lesions, (3) brain positron emission tomography scanning (PET, using FDG, or [^{18}F]2-fluoro-2-deoxyglucose) to identify regions of decreased brain metabolism usually associated with epileptic foci, and (4) neuropsychological testing to identify focal impairment of cognitive function corresponding to brain regions that give rise to seizures. A clinical summary of the study patients, including brain imaging results and clinical outcome, is provided in Table 1.

Location of seizure precursors was validated by clini-

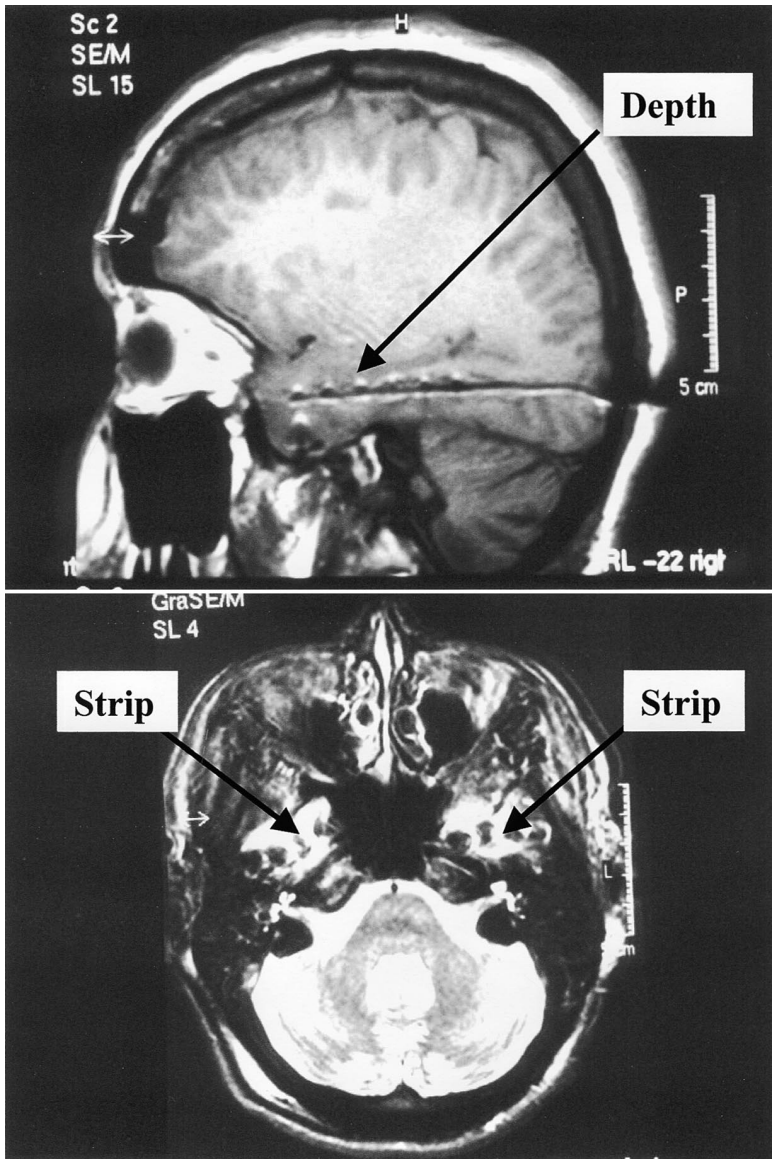

Figure 1. Long-Term Energy, Patient #1

Intracranial EEG electrode placement in patient #1, imaged on MRI scan. Subtemporal strip electrodes were placed under the temporal lobes bilaterally through burr holes through the temporal bones. Bilateral temporal depth electrodes were placed stereotaxically through burr holes in the occipital regions bilaterally.

cal outcome after epilepsy surgery in four of the five study patients (Table 1). Patient #2 chose not to have epilepsy surgery despite a majority of seizures arising from the right hippocampus. This patient had normal brain imaging and seizures that spread from one side to the other within several seconds, predicting a poorer chance of significant reduction in seizures after epilepsy surgery.

Table 2. Time between Seizures

Patient	Mean Time to Next Seizure (Hr)	Standard Deviation (Hr)	Range (Hr)
1	12.7	10.2	0.9–22.8
2	16.3	30.9	0.7–102.3
3	19.2	12.7	1.7–35.1
4	27.5	35.2	2.3–103.7
5	9.8	15.1	0.6–35.6

Spacing of seizures over time for each patient, listed as time to next seizure, with standard deviation and range of values.

Each patient had one six-contact "depth" electrode placed stereotaxically in each temporal lobe, using coordinates generated from a high-resolution MRI scan of the brain referenced to a coordinate frame fixed to the head of the patient for surgery. These electrodes were placed through a burr hole in the occipital region of the skull and advanced forward so that the most anterior contact lay in the amygdala and more posterior contacts were located along the head and body of the hippocampus. Additional electrodes were placed directly on the surface of the brain (subdural electrodes) over and under the temporal lobes bilaterally through a single burr hole made in the temporal bone on each side of the skull. Three patients (#3, #4, and #5) also had subdural electrodes placed on the surface of the frontal lobes bilaterally. Figure 1 demonstrates placement of intracranial depth and subdural temporal electrodes in one study patient.

All EEG recordings were reviewed visually by four epileptologists certified by the American Board of Clin-

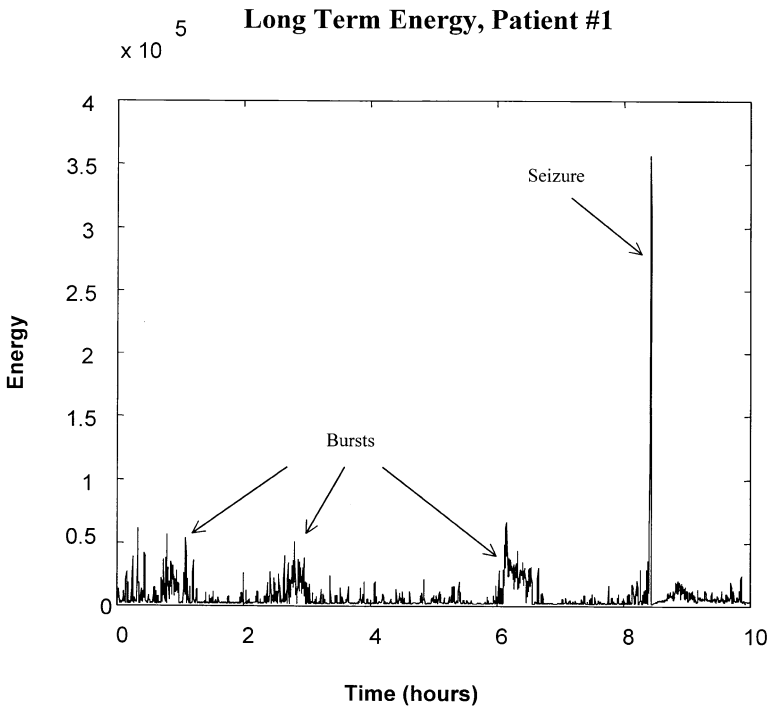

Figure 2. Long-Term Energy Burst, Raw EEG

Prolonged energy calculated from two electrodes in a bipolar montage placed proximate to the ictal onset zone prior to a single seizure in patient #1. Similar prolonged bursts of energy were seen prior to other seizures in patients #1, #3, and #4, but not during baselines.

ical Neurophysiology in EEG (BL, TH, PP, CE), for purposes of clinical decision-making. The first author visually reviewed the EEG for each seizure before quantitative analyses of these data and marked the following times: (1) the *earliest EEG change* associated with seizures: this point in time was found by identifying unequivocal seizure activity on the EEG and then moving backward in time to the point at which the first clear, sustained change from the patient's EEG baseline prior to the seizure was detected; and (2) the *unequivocal EEG onset* of seizures: this marked the time at which an EEG pattern typically associated with seizures (Risinger et al., 1989) first became unquestionably clear and could be identified independent of knowing that a seizure followed. Intracranial EEG, simultaneous video, and medical records were reviewed in their entirety for each patient. Important clinical activity, sleep-wake cycles, times, and doses of medication administered during the monitoring period were recorded and analyzed.

Results

In two patients (#1 and #4), all seizures began in one temporal lobe and earliest EEG changes were very focal, confined to one or two adjacent electrode contacts. This implies that these contacts were placed in or very close to the epileptic focus in these patients. Seizures arose independently from both temporal lobes in the remaining three patients (#2, #3, #5). Earliest EEG changes were poorly localized in patients #2 and #5, indicating either less favorable electrode placement or that seizures arose from a more diffuse area in these individuals. In patient #3, earliest EEG changes were localized after ~0.5 s demonstrating a loss of normal EEG background in the anterior hippocampal electrodes bilaterally. In all five patients, unequivocal onset of seizure activity on EEG was localized to one or two adjacent electrode contacts. Unequivocal EEG onsets of seizures were stereotyped for each patient, suggesting a reproducible, individualized pattern of initiation and spread.

Measures of energy in the EEG signal formed the core of quantitative methods used to analyze seizure-related activity (see Experimental Procedures). These were chosen because: (1) their calculation is simple and fast, consisting only of squaring the voltage at each point measured in the digital EEG and summing this up over a particular period of time; and (2) signal energy, as we defined it, is sensitive to EEG waveforms associated with seizures and epileptic foci in the brain, such as epileptiform spikes, rhythmic sharply contoured waveforms, and high-amplitude slow (0.5–4 Hz) activity seen after bursts of epileptiform activity.

In the first experiment, signal energy in the EEG was computed over the entire hospital stay in the three patients, #1, #3, and #4, who had highly localized earliest EEG changes prior to seizure onset. Mean time between seizures was 12.7 hr for patient #1 (stdev = 10.2 hr, range 0.9–22.8 hr), 19.2 hr for patient #3 (stdev = 12.7 hr, range 1.7–35.1), and 27.5 hr for patient #4 (stdev = 35.2 hr, range 2.3–103.7 hr). This information is listed for all patients in Table 2. Periodic elevations in signal energy appeared to occur in the epileptic focus intermittently throughout the hospital stay and increased in number beginning approximately 7 hr prior to seizures. Figure 2 shows a representative long-term energy plot beginning 8 hr prior to a single seizure in patient #1. The figure demonstrates several prolonged bursts of energy, some lasting more than 30 min, as seizures approach. Bursts were defined as sustained elevations of signal energy of greater than two standard deviations above the interburst baseline for periods of 5 min or more in a running average of 5 min duration. Bursts occurred in the epileptic focus region in patients #1 and #4, though substantially lower amplitude synchronous activity in

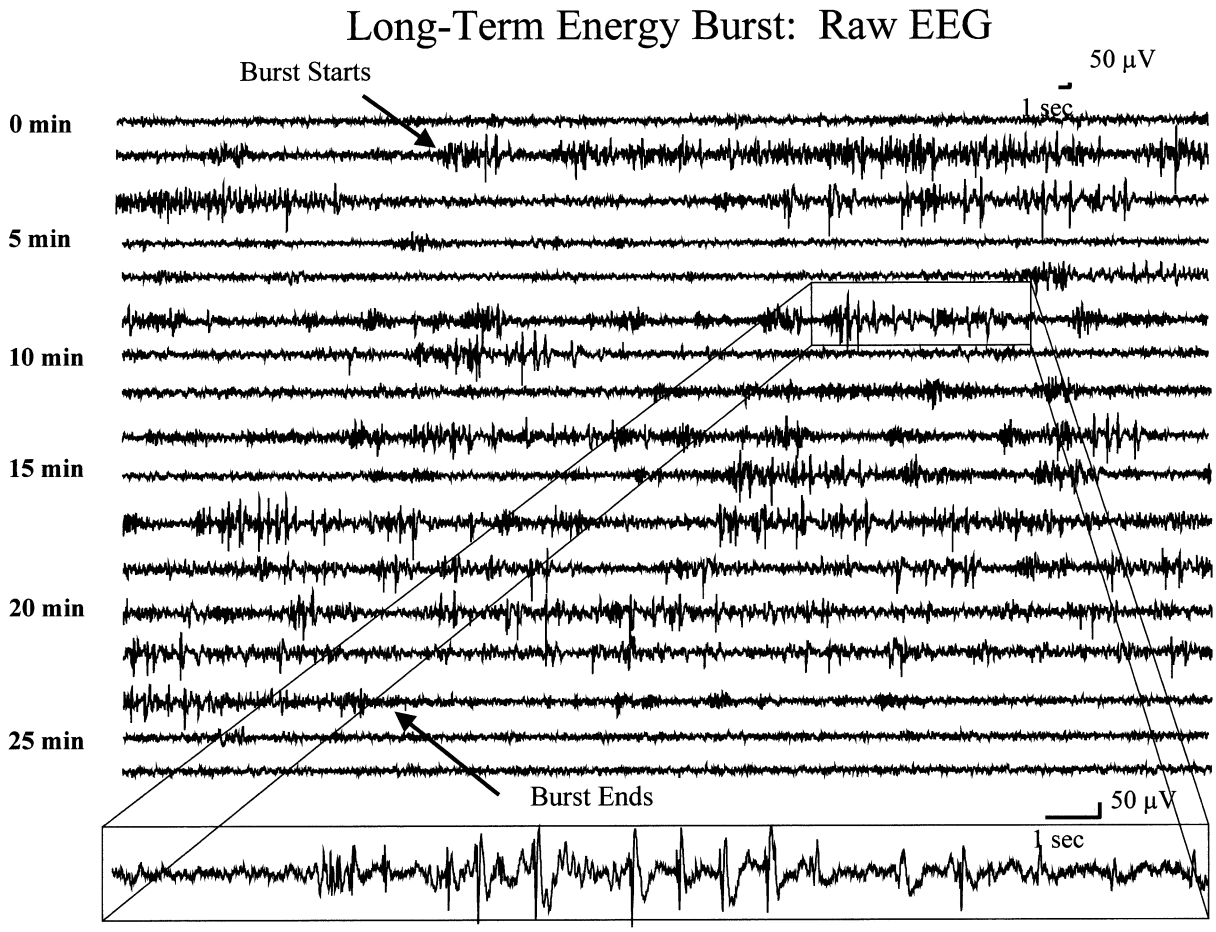

Figure 3. Number of Long-Term Energy Bursts versus Time to Seizure

Segment of 28.5 min of unprocessed EEG recorded from an electrode in the seizure onset zone in patient 1 (left hippocampus in this patient) including a period of time constituting a long-term energy burst lasting almost 25 min. Each horizontal row contains 100 s of continuous EEG. Bursting activity begins ~130 s into the record (marked by arrow, second row) and continues until the third row from the bottom (also marked). A small box is drawn around 20 s of EEG in the sixth row of EEG (9 min into the figure), which is enlarged at the bottom of the figure. This segment demonstrates typical high-amplitude epileptiform discharges and slowing that comprise long-term energy bursts.

the opposite mesial and subtemporal electrodes were often present. In patient #3, long-term energy bursts often appeared with approximately equal amplitude bilaterally, perhaps related to the independent bitemporal unequivocal EEG seizure onsets seen in this patient, but were more frequently seen in the right temporal region. Increases in long-term energy were not detected at control electrode sites in the frontal and posterior temporal lobes. Visual inspection of long-term energy bursts revealed increasingly complex spikes accompanied by high-amplitude low-frequency activity (0.5–4 Hz) and loss of normal background activity in the epileptic focus channel during these periods. Figure 3 displays raw EEG in a single channel in the epileptic focus comprising a typical long-term energy burst that occurred 4.5 hr prior to seizure onset and lasted ~25 min. The figure includes a "close-up" of typical epileptiform discharges and slow activity seen during these bursts for patient 1. Prolonged bursts of signal energy were more common while patients were asleep, as is typical of epileptiform discharges, but were not attributable to EEG patterns associated with sleep. Figure 4 demonstrates the temporal relationship between long-term energy bursts and time of onset of electrographic seizures. Bursts appeared to be concentrated between 7 hr and 30 min prior to seizure onset. Conclusions could not be drawn about the incidence of long-term energy bursts more than 12 hr prior to seizure onset, due to data inclusion criteria (see Experimental Procedures). Long-term energy was elevated after each seizure and remained increased for an average of 4–6 hr. This agrees with the findings of Franaszcuk and Bergey, who found increased synchrony in the region of the epileptic focus after seizures to the end of their 2 hr analysis period (Franaszcuk and Bergey, 1999). For this reason, long-term energy bursts could only be evaluated before the first seizure when seizures occurred less than 6 hr apart. This suggests that mechanisms giving rise to clustered seizures are likely different from those leading to isolated seizures. These findings suggest that seizure generation may begin far earlier than 1 hr prior to clinical seizures.

In a second observation, patient #1 demonstrated stereotyped 6–12 s runs of very focal, rhythmic, high-frequency activity in the left anterior hippocampus (the

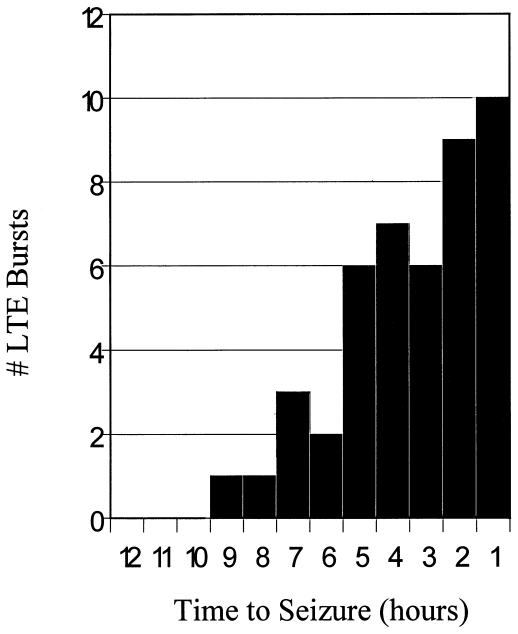

Figure 4. Number of Long-Term Energy (LTE) Bursts versus Time to Seizure (Ten Seizures, Three Patients)

Time of occurrence of long-term energy bursts in relation to seizure onset is displayed for patients #1, #3, and #4. There was no clear relationship between burst amplitude or duration and time to seizure onset. Epochs of data not meeting inclusion criteria (e.g., at least 12 contiguous hr without interruptions of 5 min or more by artifact or gaps in the data) were not analyzed, due to the lack of ability to determine if these data epochs led to or followed subclinical seizures. Because of these strict inclusion criteria, and frequent seizures and clusters induced by medication taper, little information is available about the incidence of long-term energy bursts at times greater than 12 hr prior to electrical seizure onset. These findings support the hypothesis that increasing incidence of long-term energy bursts appear to correlate in time with approaching electrographic seizures beginning ~7 hr before seizure onset.

focus in this patient) just prior to seizures. Each of these runs of activity began abruptly at 20–25 Hz then gradually increased in amplitude while slowing to 6–10 Hz, sometimes spreading to adjacent electrodes before either leading to seizure onset or ending in higher amplitude, irregular 1–2 Hz activity. Typical examples of these discharges are displayed in Figure 5, prior to the patient's first seizure. These discharges were consistent with brief, highly localized seizures on EEG, but did not cause any clinical symptoms. Inspection of the patient's entire 4 day intracranial EEG recording demonstrated that these electrical events clustered around clinical seizures and were extremely rare at other times. Figure 6 demonstrates the rate of occurrence of these brief, very focal "subclinical seizures" in relation to unequivocal electrical onset of the patient's six typical seizures. The majority of these 37 electrical events occurred within 2 hr of seizure onset. Discrete, self-limited, subclinical seizures in intracranial EEG recordings are reported to have important value in identifying the location of the epileptic focus in patients with mesial temporal lobe epilepsy (Sperling and O'Connor, 1990; Schiller et al., 1998; Schuh et al., 2000). Their timing, predictive value, and potential role in seizure generation have not been reported previously. Of note, two of the patient's six seizures, which were excluded from the accumulated energy experiment (below) because the EEG was briefly obscured by artifact in the 3 hr leading up to seizure onset, were included in the above analysis.

In a third experiment, "accumulated energy"—a running sum of the square of the EEG voltage sampled at 200 Hz—was calculated from EEG data beginning 50 min prior to unequivocal seizure onset on EEG and ending 10 min after onset. Accumulated energy was computed at the electrode site recording the earliest or maximal (if several contacts were involved simultaneously) unequivocal EEG onset for each seizure. This was compared to two controls: (1) baseline controls: randomly chosen, 1 hr EEG segments recorded from the seizure focus, but separated from the beginning or end of any seizure by at least 3 hr of uninterrupted, artifact-free EEG, and (2) contralateral controls: data acquired during epochs leading up to seizures but from analogous electrodes in the temporal lobe opposite the seizure focus. Seizures and baseline data were compared only within the same state of consciousness (e.g., awake versus asleep), as baseline energy was found to be higher during sleep than wakefulness, due to normal EEG waveforms occurring during sleep (Table 3).

80 1 hr EEG epochs were analyzed: 30 leading to seizures, and 50 baselines. Figure 7 displays all baseline and preseizure epochs recorded from the seizure focus in all five patients, normalized to include both sleep and awake records for all subjects. For each patient, accumulated energy during baseline periods was very similar (dashed red lines) and accumulated energy in preseizure recordings (solid blue lines) clearly rose above these baselines within 50 min prior to seizure onset. Table 3 displays "preseizure declaration times" calculated for each patient. This was defined as the time prior to seizure onset at which each accumulated energy curve for a particular patient crossed the level of the highest baseline accumulated energy for that patient. Using this simple threshold function, data epochs were correctly classified as either preseizure or baseline with 89% accuracy, a sensitivity of 90%, and specificity of 88%. The choice of optimal threshold by using this method was verified by experimentally generating a receiver-operating characteristic curve (Figure 8), plotting sensitivity versus one minus specificity for a wide range of threshold values. Mean time from declaration of impending seizure to unequivocal EEG onset of seizures by this simple algorithm was 18.5 min (±13.4 min). Close examination of Figure 7 demonstrates that accumulated energy actually rose above baselines much earlier than this time in many cases. This suggests that it should be possible to devise classification algorithms, perhaps more sophisticated than a simple linear threshold, capable of identifying preseizure epochs even farther in advance of electrical seizure onset than the above results. These findings complement reports of "seizure anticipation" using "nonlinear analysis" 2–6 min prior to seizure onset in 17 of 19 patients by Martinerie et al. (1998), Le Van Quyen et al. (2001), and in 20 seizures processed by Lehnertz and Elger (1998).

Baseline signal energy was increased following clusters of two or more seizures within a 6 hr period. When this was taken into account, four EEG epochs following

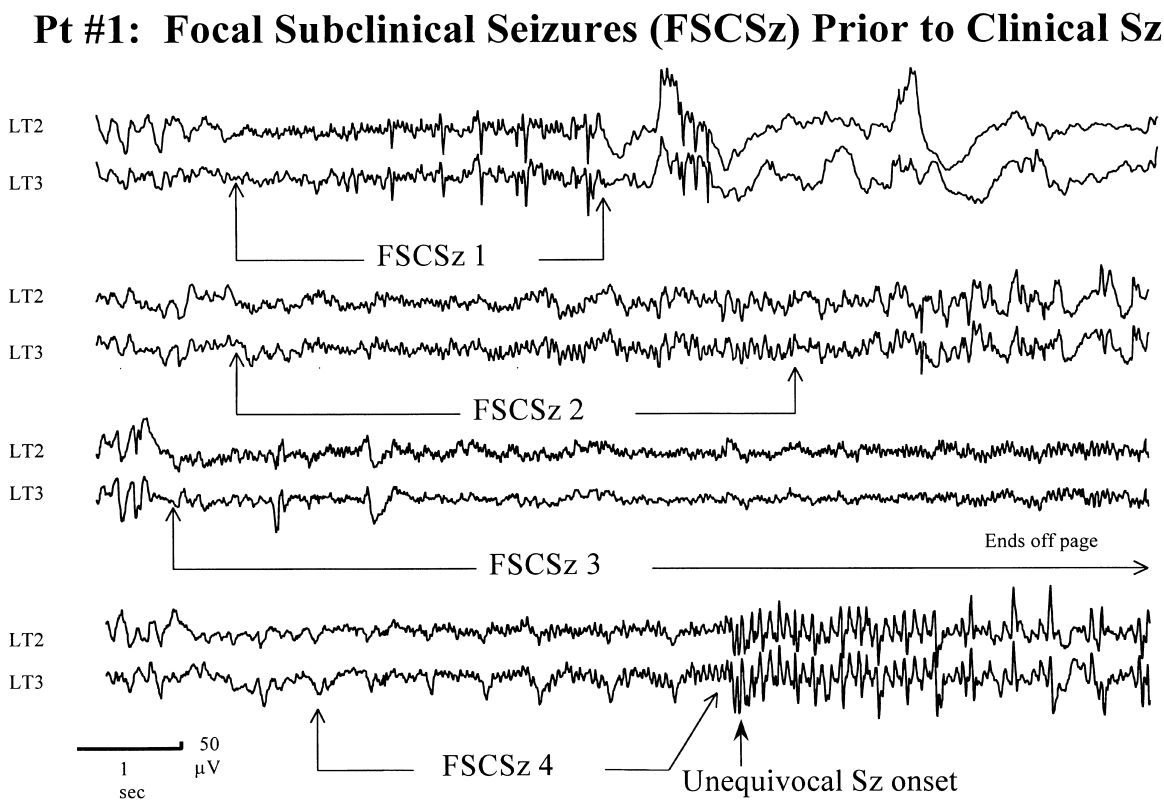

Figure 5. Rate of Subclinical Seizures versus Time to Electrical Onset of Symptomatic Seizures

Focal subclinical seizures prior to one seizure of patient #1 recorded from left hippocampal depth electrode contacts LT2 and LT3 referenced to a remote electrode. These electrical events began with stereotyped fast activity and were of variable length. The last subclinical seizure, #4, leads to a clinical seizure with UEO marked by the arrow. Subclinical seizures did not occur within 6 hr after electrographic seizures except when seizures clustered together over short periods of time. There was no evidence that these discharges were associated with the postseizure period.

clusters initially mislabeled as "preseizure" were correctly reclassified as baselines, improving overall accuracy to 94%. There were no clear EEG changes responsible for the two remaining false positive declarations; however, these could have occurred during prolonged long-term bursts of energy between seizures (see above), or asymptomatic seizures hidden by gaps in recorded data found more than 3 hr prior to these baseline segments. There were no specific characteristics or obvious systematic errors to account for misclassification of three false negative epochs. The short prediction horizon for patient #4 sets him apart from the other study patients, as does the unusually short time delay between electrical and clinical seizure onset in this patient. These findings are of unclear significance.

In patients with seizure onsets confined to one temporal lobe (#1, #4), and in two of the patients with seizures arising independently from both temporal lobes (#2, #5), increased accumulated energy was found only on the same side as unequivocal EEG onset for each seizure. In patient #3, of the seven seizures that met inclusion criteria, unequivocal EEG onset was seen in the right temporal lobe for five events and on the left side in the other two. Pre-seizure changes in accumulated energy predicted onset on the right side for all seizures. These findings suggest that the epileptic focus, or region critical to generating seizures in patient #3 was likely located in the right hemisphere, perhaps near pathways allowing rapid conduction or diversion of activity to the left hippocampus under some circumstances. This hypothesis is supported by the patient's seizure-free outcome after surgical removal of the right temporal lobe.

Visual inspection of preseizure EEG recordings did not demonstrate obvious findings that corresponded to changes in accumulated energy. The actual number of epileptiform discharges (spikes) during the 50 min before seizures did not differ statistically from baseline periods, in agreement with Lange et al. (1983) and Katz et al. (1991). The frequency of these discharges during longer periods prior to seizure onset and their correlation with impending seizures was not analyzed. Changes in accumulated energy were not clearly confined to a particular frequency band in the EEG.

Further analyses were performed to determine if high-amplitude epileptiform activity during long-term energy bursts or focal subclinical seizures accounted for the rise in accumulated energy prior to clinical seizures. Long-term energy bursts occurred prior to 8 of 30 seizures during the 50 min before unequivocal electrographic seizure onset in which the accumulated energy was calculated. Given that accumulated energy was elevated above threshold prior to seizure onset in 27 of

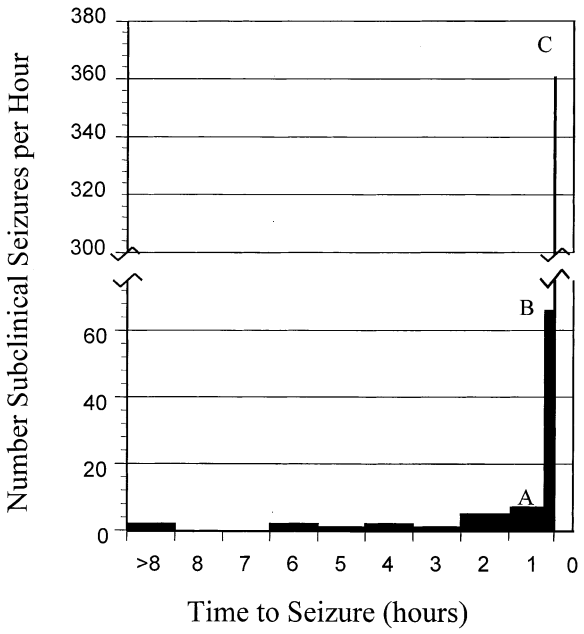

Figure 6. Focal Subclinical Seizures Prior to Clinical Seizure #1

Rate of occurrence of subclinical seizures versus time to electrical seizure onset for patient #1: the rate of occurrence of subclinical seizures relative to time of unequivocal electrographic onset (UEO) of seizures is displayed. Rates are normalized to the number of events per hour. The graph demonstrates that beginning ~2 hr prior to UEO, there is marked increase in the occurrence of subclinical seizures. This increase rises dramatically beginning in the period 50–10 min prior to UEO (A) and more in the period 10–1 min prior to UEO (B). The rate of occurrence rises most dramatically within 1 min (C) prior to electrical seizure onset. Subclinical seizures were rarely more than 3 hr removed from seizures.

these 30 epochs, it was felt that long-term energy bursts alone could not account for preseizure changes in accumulated energy. To examine the contribution of focal subclinical seizures to accumulated energy, energy generated by this activity was subtracted from the accumulated energy calculation each time one of these events was detected, substituting the energy from the adjacent previous EEG segment during these time periods. There was no significant difference in the accumulated energy tracings before and after removal of energy due to subclinical seizures, when comparing plots of these curves on the same graph. When the two curves were compared quantitatively for each preseizure period in this patient, an average difference of $<3.5\%$ in accumulated energy was found between these curves at any given point. This difference was not felt to be clinically significant and did not significantly alter preseizure declaration times. These findings suggest that the buildup in accumulated energy in the 50 min prior to seizures cannot be accounted for solely by changes in long-term energy or the presence of subclinical seizures.

Discussion

These results are important for several reasons. First, they demonstrate that there are changing forms and amounts of abnormal electrical activity in the epileptic focus that increase over long periods of time as seizures approach. Second, they give hints to the mechanisms underlying seizure generation and their time course. Third, they provide important insight into the experimental design, data collection, and processing required for seizure prediction trials. Finally, these results may be exploitable in an implantable, therapeutic device. It is important to point out that these results do not constitute genuine seizure prediction, which would require a prospective analysis of data when time to seizure is unknown. This study is currently under way. Rather, they provide evidence for a series of reproducible events comprising seizure generation and a means for measuring them that may make it possible to reliably predict seizures.

Mechanisms

Our findings suggest that seizure generation may be a multistage process that evolves over hours. Intermittent bursts of energy in the epileptic focus, when influenced by factors that promote seizures, may become more common and then give rise to brief, localized subclinical seizures. As these rhythmic discharges occur more frequently, adjacent tissue is recruited, increasing accumulated energy and heralding oncoming seizures. This agrees with reports of increasing coherence in chaotic parameters near the seizure focus during the preseizure period (Iasemidis et al., 1996, 1997).

Numerous mechanisms might account for these findings, likely generated by hypersynchronous synaptic as well as intrinsic voltage-dependent currents with longer time constants (Dichter and Ayala, 1987). Internal factors, such as sleep deprivation and hormone levels may modulate bursts of localized epileptiform activity. Neu-

Table 3. Accumulated Energy: Number of Records, Classification, and Prediction

Patient Number	Mean Preseizure Declaration Time (Min)	Stdev of Pred Time (Min)	False Negatives	False Positives	Seizures		Baselines	
					Asleep	Awake	Asleep	Awake
1	23.3	15.25	1	3	1	3	6	6
2	20.78	15.77	1	2	2	2	6	4
3	17.29	10.15	0	0	1	6	5	4
4	1.3	1.83	1	0	2	3	4	5
5	21.89	11.61	0	1	7	3	4	6
All Patients	18.49	13.42	3	6	13	17	25	25

Mean prediction horizon, standard deviation, and number of false positive and false negative predictions are displayed for each patient, in addition to the number of seizure and baseline epochs and their distribution between wakefulness and sleep.

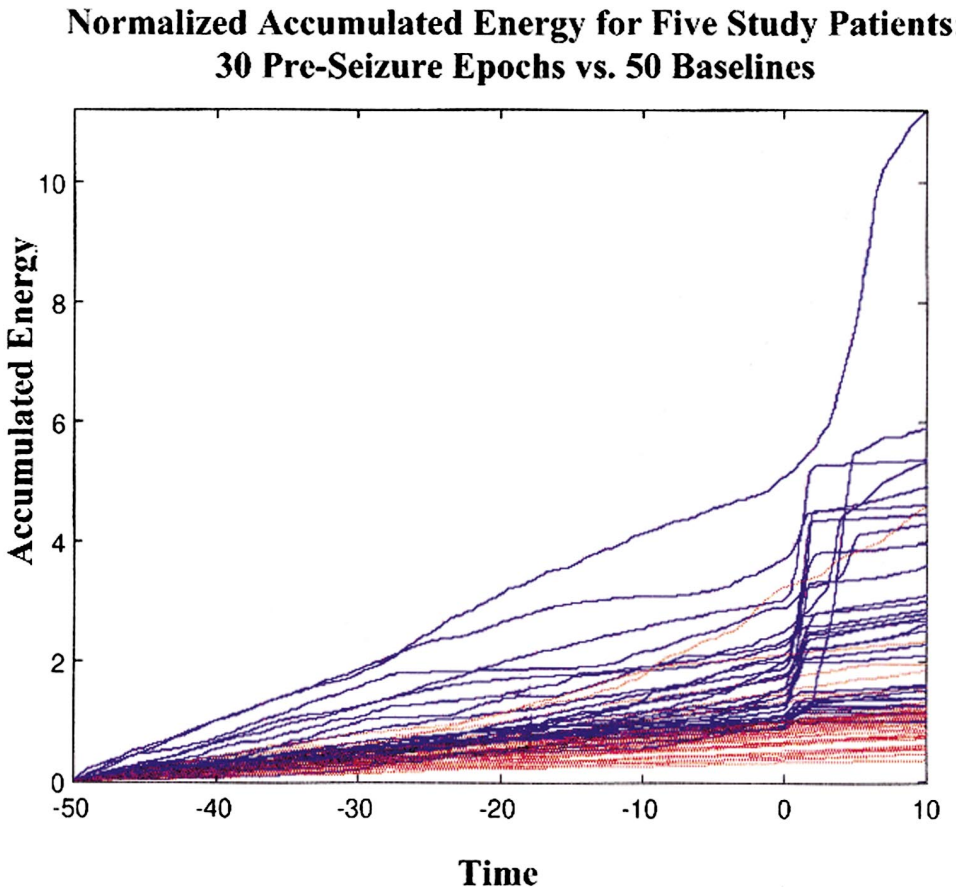

Figure 7. Normalized Accumulated Energy for Five Study Patients

Accumulated energy trajectories for all five patients, including 30 preseizure and 50 baseline epochs. Data are normalized within patients to include both sleep and awake epochs. Baseline accumulated energy trajectories (dotted red lines) cluster together at the bottom of the figure. Preseizure trajectories (blue lines) deviate from baselines within 50 min prior to seizures, though a number of the preseizure epochs demonstrate deviation from baseline trajectories already in progress at 50 min prior to seizure onset, suggesting earlier preseizure change. Time = 0 marks unequivocal electrographic seizure onsets, marked by the first author, according to standard clinical criteria.

ronal excitability could be enhanced by slow accumulation of extracellular K^+ (Dichter et al., 1972), alkalinization (Tang et al., 1990), or changes in intracellular osmolarity (Schwartzkroin et al., 1998), which could effect slow potentiation of excitatory synapses via local electrical coupling or neuromodulatory substances. Changes in the redox state of the focus related to altered perfusion, O_2 extraction or neuronal activity has been shown to significantly affect NMDA receptor activity. Increases in energy could also trigger transcriptional changes in neurons within the epileptic focus. The resulting gene products may initiate a cascade of intracellular changes leading to seizure onset (Liang and Jones, 1997). This idea is appealing, because communication between cell surface membrane and the nucleus may require minutes and sometimes hours to occur. In addition, long-term potentiation is known to influence gene transcription, providing one potential mechanism for electrical activity at the synapse to affect protein expression (Bailey et al., 1996). These events could be analogous to changes that occur in cortical neurons when memories are stored.

Although speculative, these hypotheses are testable, and the corresponding processes could be modified prior to seizure onset, leading to specific, targeted new therapies. Our findings, for the first time, suggest the need to evaluate these processes in broader time windows.

The Next Experimental Steps

Because collection of human data is ethically limited to clinical necessity, we are employing animal models of human temporal lobe epilepsy in an attempt to understand the preseizure cascade. Some models, such as systemically delivered pilocarpine and sustained electrical status epilepticus, cause widespread neuronal injury. Others, such as intrahippocampal injection of kainic acid, are more focal. All are problematic because the frequency and severity of associated seizures is difficult to control. Genetically engineered animal models of epilepsy (i.e., knockouts) are less variable, though most are more similar to human primary generalized epilepsy than to seizures of focal origin (Noebels et al., 1990; Noebels and Rutecki, 1990; Burgess and Noebels, 1999; Noebels, 1999). Transgenic mouse epilepsy models may be transferable to primates (Kafri et al., 2000; Wang et al., 2000),

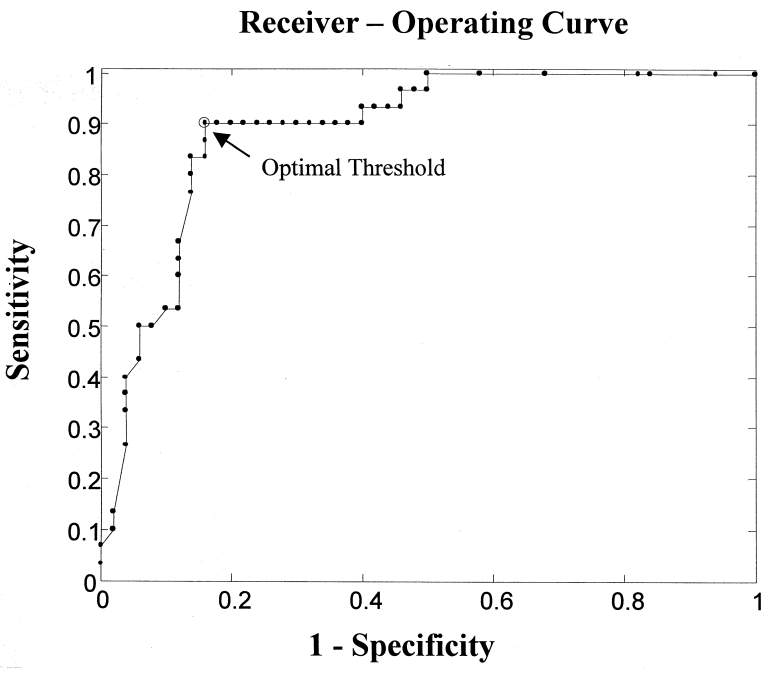

Figure 8. Receiver-Operating Characteristic Curve

The empirical receiver-operating characteristic curve (ROC) graph compares performance of seizure prediction sensitivity and specificity based upon accumulated energy as a function of raising and lowering the prediction threshold (see Figure 7). Each point on the curve corresponds to a different threshold. The vertical axis of this graph represents the sensitivity of prediction based upon accumulated energy and is plotted against 1-specificity of the prediction algorithm at that specific threshold value. In a practical sense, points at the bottom left corner of the curve represent performance for thresholds at which there are no false alarms, and none of the seizures can be predicted. Positions at the top right corner represent thresholds at which all seizures are predicted, but all baselines are false alarms as well. An ideal detector has a curve that goes from the bottom left corner to the top left and then from the top left to the top right (two perpendicular lines). If a classifier produces an ROC curve that is a diagonal line, this implies that the system randomly classifies data segments as preseizure or baseline with error probabilities that sum to one. The threshold chosen for the accumulated energy seizure prediction algorithm described above (circled point) is demonstrated to be optimal for this system, given its place at the "corner" of the ROC curve.

offering potential benefits for preclinical testing of algorithms and implanted devices.

Clinical Research: Experimental Issues

All tapes were reviewed in their entirety to screen out artifacts and gaps in EEG data, which necessitated excluding some epochs from analysis (see Experimental Procedures). In retrospect, strict review and inclusion criteria were justified, given our findings that postseizure elevations in EEG signal energy lasted up to 6 hr and that a large percentage of apparent "false positive" precursors occurred in anticipation of previously unrecognized subclinical seizures. These findings reinforce the need for long, continuous, and complete data sets that are as free as possible from artifacts and recording gaps for this type of research.

All study patients underwent rapid tapering of their antiepileptic drugs to precipitate seizures, which is standard during presurgical evaluation, and facilitates seizure clustering. Haut et al. have demonstrated that clustered seizures demonstrate different EEG characteristics than single spontaneous seizures in the same patient (Haut et al., 1997). Studies of seizure precursors in the absence of medication withdrawal will be important to validate prediction algorithms for application outside of the monitoring setting.

Accumulated energy measurements were only useful in separating preseizure from baseline epochs when state of consciousness was taken into account. Other investigators have dealt with this issue by examining seizures only during wakefulness. Future trials will need to account for EEG changes during all states of awareness.

Though some of the variability in findings between our five study patients is likely due to electrode placement and clinical factors, each subject was found to have a unique preseizure electrophysiology. Our experience suggests that individual variability will likely fall within a small number of pre-ictal patterns, analogous to seizure onset patterns recorded from depth electrodes in temporal lobe epilepsy (Spencer et al., 1992). This implies that prediction algorithms will likely need to be individually optimized, though utilizing a limited number of adjustable parameters.

All of the findings described in this study refer to temporal and not extratemporal epilepsy, a discussion of which is beyond the scope of this paper.

An Implantable Diagnostic-Therapeutic Device

Understanding mechanisms of seizure generation will ultimately produce the best therapies, however, an implantable antiseizure device is a natural interim goal. Figure 9 displays a schematic of such a device, based upon algorithms we have developed to predict seizures and trigger therapy as they approach. The device continuously monitors features extracted from the intracranial EEG and computes the probability of an approaching seizure, while continuously checking for electrical seizure onset. A wavelet neural network is trained, and its performance individually optimized, based upon multiple features extracted from continuous data containing both seizures and long seizure-free and preseizure intervals. The patient or physician sets the probability thresholds and rate of rise that will trigger a warning or intervention.

Electrical stimulation and local drug infusion are two

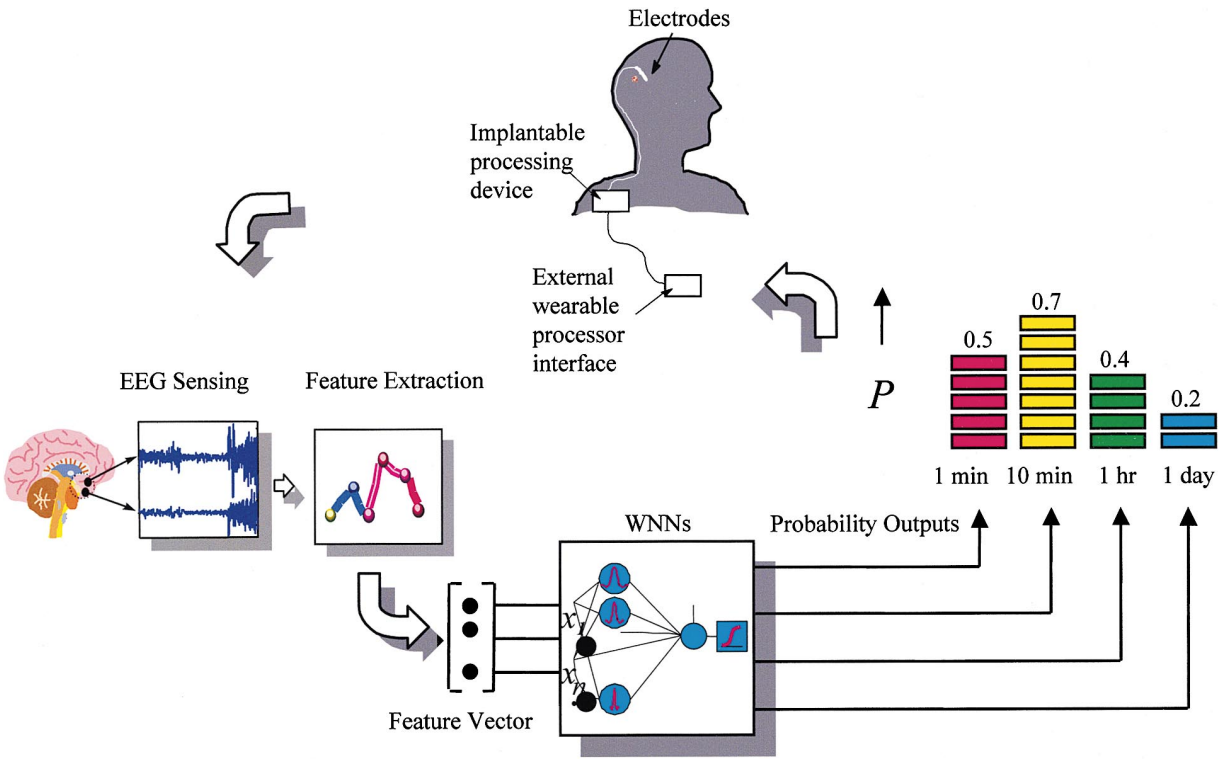

Figure 9. A Seizure Prediction Device

A schematic of an implanted device for seizure prediction and intervention. EEG is recorded from electrodes implanted in the area of the seizure focus. Instantaneous features, such as signal energy, and historical features, such as the time of the last subclinical seizure, are recorded. A neural network compares the behavior of these parameters to known behavior leading up to seizures for the given subject and continuously outputs the probability that a seizure will occur over four time horizons: 1 day, 1 hr, 10 min, and 1 min. A warning of impending seizure or intervention in the form of electrical stimulation or infusion of drugs in the area of the seizure focus are triggered when the probability of an oncoming seizure, or the increase in probability over time, exceeds a predetermined threshold value.

main therapies being investigated in conjunction with these devices. As we envision this, when seizures approach with low probability, lower amplitude stimuli that are less likely to disrupt normal brain function might be applied. Algorithms might include standard or "chaos control" pacing (Glanz, 1994; Lopes da Silva et al., 1994; Heffernan, 1996), low-level depolarization or hyperpolarization of the focus region. As the probability of seizure onset increases, stimulation intensity, duration, and area are increased, perhaps extending to subcortical structures, which may modulate seizure generation. Care must be taken to avoid stimuli that might cause tissue injury or promote kindling of seizures in otherwise healthy tissue (Lothman and Williamson, 1994). Of interest, peripheral nerve stimulation and applying magnetic fields to brain also hold therapeutic promise for treating seizures (Fanselow et al., 2000; Gluckman et al., 2001).

Infusing small amounts of antiepileptic drugs locally in the epileptic focus may also inhibit seizure generation. Candidate drugs for infusion include benzodiazepines, lidocaine, standard, or newer antiepileptic agents. This approach has been the subject of considerable interest for the past several years (Eder et al., 1997; Ward and Rise, 1998; Stein et al., 2000).

Analogy to Cardiology

Intelligent devices to treat seizures may prove more difficult to implement than those used to treat cardiac arrhythmias. Implantable cardiac defibrillators process one channel of data, detect arrhythmias after their onset, and deliver graded shocks to "reset" the heart's electrical system. Side effects such as pain and alteration or loss of consciousness are accepted, since the goal of therapy is to preserve life. Epilepsy devices will likely require processing multichannel data in parallel, with the goal of preventing clinical symptoms, such as loss of awareness. Delaying therapy until electrical seizures are detected may be too late to prevent clinical symptoms, given the rapidity with which seizures may spread. Finally, epilepsy devices will likely require optimization for each patient, and perhaps periodic retraining, given the potential for seizures and electrical stimulation to alter network dynamics in the brain over time.

Conclusion

Our results suggest that the changes in cellular and network function that lead to epileptic seizures likely develop over hours, providing exciting clues to potential mechanisms underlying seizure generation. Understanding these mechanisms should produce new, more effective and specific therapies for epilepsy. Our results also suggest that seizures in mesial temporal lobe epilepsy are predictable within time horizons that make it possible to prevent them, opening an immediate opportunity to develop intelligent, implantable therapeutic devices.

As seizure precursors become better understood, it may become possible to trace the earliest precursors of seizures back to their site(s) of origin, perhaps enabling ablation of critical regions of abnormal function by minimally invasive surgery or other techniques to replace large-scale brain resections that are now standard. Most important, these results provide new neurophysiologic evidence that may bring researchers closer to understanding how epilepsy begins and perhaps how to prevent it.

Experimental Procedures

Continuous intracranial EEG and video were collected using a digital, 64-channel, 12 bit Nicolet BMS-5000 epilepsy monitoring system and were stored on videotape. Referentially recorded EEG was downloaded from tape and archived to CD-ROM for processing. EEGs were digitized at 200 Hz and recorded after filtering through a bandpass of 0.1–100 Hz. Data were processed using a combination of MATLAB programs and custom-written C++ code for more prolonged, computationally intensive tasks on a network of four 410 MHz IBM personal computers running Windows NT and equipped with parallel processors. Hospital stays varied from 3–14 days in the five study patients, yielding roughly 50 gigabytes of raw data available for processing. Bipolar electrode montages were used to eliminate common mode artifact. A digital 60 Hz notch filter was employed to eliminate line noise. Videotapes were watched in their entirety for clinically important events, and approximation of periods of sleep and wakefulness. Finer resolution of sleep-wake cycles was achieved by examining the EEG.

Strict inclusion criteria were used in the study of long-term energy to ensure that the relationship between long-term energy bursts and seizures could be properly explored. Seizures that occurred with less than 6 hr between them were excluded from analysis, except for the first seizure in each cluster. In addition, all processed data segments had to be preceded and followed by at least 6 hr of uninterrupted, contiguous EEG, containing no artifacts or gaps of 5 min duration or longer. These strict criteria resulted in elimination of approximately 1/3 of baseline and preseizure data from the analysis in the three patients evaluated in this portion of the study.

In the study of accumulated energy, all preseizure epochs meeting criteria for inclusion were used. Acceptable baseline epochs were divided into hour-long segments, assigned numbers, and then randomly selected for analysis. To be accepted, preseizure and baseline epochs had to be preceded by at least 3 hr of uninterrupted data, excluding brief artifacts lasting less than 10 s. This excluded 14 preseizure epochs from processing. A 15th seizure that arose outside of the temporal lobes (patient #5) was not included in the analysis. Not all excluded data epochs were rejected due to artifact. Some occurred near the beginning or end of a tape where previous or trailing data were lost, interrupted, or obscured. Additionally, only one baseline epoch was allowed from a single 3 hr period, to eliminate biasing results. Baseline epochs had to be recorded at least 80% during sleep or wakefulness. Target numbers for baselines were arbitrarily set at six each collected during sleep and wakefulness for each patient in this study. Table 3 demonstrates all usable, randomly chosen baseline segments available for processing, using the stringent selection criteria listed above.

Calculation of Signal Energy and Accumulated Energy

Signal energy was calculated in a sliding window of 1.25 s to assure signal stationarity, chosen empirically, based upon the work of Qin (1995). The instantaneous energy was obtained by squaring each value of the intracranial EEG sequence as follows:

$$E_i[n] = x^2[n], \tag{1}$$

where $x[n]$ is the n^{th} value of the intracranial EEG signal in the focus channel within the i^{th} time window, indexed by time. Average energy values were computed by averaging every 250 points (indexed by n in Equation 1 above), equivalent to 1.25 s of the instantaneous energy at the given sample rate of 200 Hz. A sliding rectangular window was used to process the data.

Average energy values were computed by averaging every 250 points, equivalent to 1.25 s of the instantaneous energy at the given sample rate of 200 Hz. Results were computed in a moving average, overlapping consecutive calculations by 0.8 s (160 points) to give a higher resolution. This was accomplished by shifting the computation window in Equation 2 0.45 s (90 points) each time:

$$E_k = \frac{1}{N} \Sigma\, x^2[n], \tag{2}$$

where E_k represents the k^{th} value of the average energy over a window of 250 points, N is the total number of instantaneous energy values averaged, in this case $N = 250$.

A second level of averaging was performed to calculate the accumulated energy. Ten consecutive values of the average energy are added, divided by 10, and then added to the running tally of accumulated energy. This process is equivalent to integrating the absolute value of the EEG voltage as it is recorded on the intracranial EEG. An overlap of 50%, or five points, is used in this measure, again to improve resolution in time. Equation 3 summarizes how each accumulated energy value is obtained:

$$AE_m = \frac{1}{10} \Sigma\, E_k + AE_{m-1}, \tag{3}$$

where AE_m is the m^{th} value of the accumulated energy, AE_{m-1} is the $m^{th} - 1$, or previous value, of the accumulated energy.

Accuracy Calculation

Classification accuracy was calculated as the percentage of total number of correct predictions with respect to total number of records analyzed (Echauz et al., 1998):

$$A = 100\left[1 - \frac{1}{N} \sum_{i=1}^{N} |y_i - \hat{y}_i|\right], \tag{4}$$

where A is the percentage of accurately classified data epochs, where y_i, is the true classification of the i^{th} record (1 = preseizure, 0 = baseline), $\hat{y}_i$ is the i^{th} system's classification of the same event (1 = preseizure, 0 = baseline), and N is the total number of records classified.

Data Handling and Processing

The large computational burden of these experiments required adopting a system of procedures to deal with the more than 100 CDs, each containing 480 MB of digital data, processed for the above experiments. A custom toolbox of programs, written in MATLAB and C++ was developed, with an emphasis on flexibility, automation of feature extraction from raw data, and tabulation of results. Two major groups of programs were developed: generic programs that were run on all data sets, including feature extraction, window length adjustment, and data shifting routines; and patient-specific programs used to generate a set of individual features for each data epoch and to compile results for each trial. Batch programs were generally run overnight on the network, and results were automatically saved into patient-specific work folders labeled by patient number. Of great importance, descriptive naming conventions were established for each feature generated from each patient's data, for each data epoch, for different states of consciousness, and for different data classes (preseizure, baseline, control channels, etc.). These naming conventions were vital to handling the enormous amount of data processed for this study. Other issues, such as organization and control of access to the CD library of raw data, organization of files on computer hard disk drives, and assembling descriptive logs of clinical and quantitative data for each patient were labor intensive, but essential to maintaining easy access to raw and preprocessed data, calculated features, and overall results.

Acknowledgments

This work is supported by funding from the Whitaker Foundation, Epilepsy Foundation, American Epilepsy Society, University of Pennsylvania Research Foundation, Jim Jacoby, and the National Institutes of Health grant #MH-62298RO1. Drs. Litt, Esteller, Echauz,

and Vachtsevanos are founders of a small company, IntelliMedix, which supports this research. The authors express their appreciation to Steven Cranstoun, Peter Crino, Francisco Gonzalez-Scarano, Steven Scherer, Dasakumar Navaratnam, Leif Finkel, and David Raizen for reviewing this manuscript.

Received February 1, 2000; revised February 8, 2001.

References

Bailey, C.H., Bartsch, D., and Kandel, E.R. (1996). Toward a molecular definition of long-term memory storage. Proc. Natl. Acad. Sci. USA *93*, 13445–13452.

Burgess, D.L., and Noebels, J.L. (1999). Single gene defects in mice: the role of voltage-dependent calcium channels in absence models. Epilepsy Res. *36*, 111–122.

Dichter, M., and Spencer, W.A. (1969a). Penicillin-induced interictal discharges from the cat hippocampus. I. Characteristics and topographical features. J. Neurophysiol. *32*, 649–662.

Dichter, M., and Spencer, W.A. (1969b). Penicillin-induced interictal discharges from the cat hippocampus. II. Mechanisms underlying origin and restriction. J. Neurophysiol. *32*, 663–687.

Dichter, M.A., Herman, C.J., and Selzer, M. (1972). Silent cells during interictal discharges and seizures in hippocampal penicillin foci. Evidence for the role of extracellular K^+ in the transition from the interictal state to seizures. Brain Res. *48*, 173–183.

Dichter, M.A., and Ayala, G.F. (1987). Cellular mechanisms of epilepsy: a status report. Science *237*, 157–164.

Echauz, J., Kim, S., Ramani, V., and Vachtsevanos, G. (1998). Neurofuzzy approaches to decision making: a comparative study with an application to check authorization. Journal of Intelligent and Fuzzy Systems *6*, 259–278.

Eder, H.G., Stein, A., and Fisher, R.S. (1997). Interictal and ictal activity in the rat cobalt/pilocarpine model of epilepsy decreased by local perfusion of diazepam. Epilepsy Res. *29*, 17–24.

Engel, J., Jr. (1987). Outcome with respect to seizures. In Surgical Treatment of the Epilepsies, J. Engel, Jr., ed. (New York: Raven Press), pp. 553–571.

Fanselow, E., Reid, A., and Nicolelis, M. (2000). Reduction of pentylenetetrazole-induced seizure activity in awake rats by seizure-triggered trigeminal nerve stimulation. J. Neurosci. *20*, 8160–8168.

Feindel, W., Penfield, W., and Jasper, H. (1952). Localization of epileptic discharge in temporal lobe automatism. Trans. Am. Neurol. Assoc. *77*, 14–17.

Franaszcuk, P., and Bergey, G. (1999). An autoregressive method for the measurement of synchronization of interictal and ictal EEG signals. Biol. Cybernet. *81*, 3–9.

Glanz, J. (1994). Do chaos-control techniques offer hope for epilepsy? Science *265*, 1174.

Gluckman, B., Nguyen, H., Weinstein, S., and Schiff, S. (2001). Adaptive electric field control of epileptic seizures. J. Neurosci. *21*, 590–600.

Gotman, J. (1987). Computer analysis of the EEG in epilepsy. In Methods of Analysis of Brain Electrical and Magnetic Signals: EEG Handbook, A. Gevins and A. Rémond, eds. (Amsterdam: Elsevier), pp. 171–204.

Gotman, J. (1991). Relationships between interictal spiking and seizures: human and experimental evidence. Canadian J. Neurol. Sci. *18*, 573–576.

Haut, S.R., Legatt, A.D., O'Dell, C., Moshe, S.L., and Shinnar, S. (1997). Seizure lateralization during EEG monitoring in patients with bilateral foci: the cluster effect. Epilepsia *38*, 937–940.

Heffernan, M.S. (1996). Comparative effects of microcurrent stimulation on EEG spectrum and correlation dimension. Integr. Physiol. Behav. Sci. *31*, 202–209.

Iasemidis, L.D., Sackellares, J.C., Zaveri, H.P., and Williams, W.J. (1990). Phase space topography and the Lyapunov exponent of electrocorticograms in partial seizures. Brain Topogr. *2*, 187–201.

Iasemidis, L., Olson, L., Savit, R., and Sackellares, J. (1994). Time dependencies in the occurrences of epileptic seizures: a nonlinear approach. Epilepsy Res. *17*, 81–94.

Iasemidis, L., Pappas, K., Gilmore, R., Roper, S., and Sackellares, J. (1996). Preictal entrainment of a critical cortical mass is a necessary condition for seizure occurrence. Epilepsia *37*, 90.

Iasemidis, L., Gilmore, R., Roper, S., and Sackellares, J. (1997). Dynamical interaction of the epileptogenic focus with extrafocal sites in temporal lobe epilepsy (TLE). Ann. Neurol. *42*, 429.

Kafri, T., van Praag, H., Gage, F.H., and Verma, I.M. (2000). Lentiviral vectors: regulated gene expression. Mol. Ther. *1*, 516–521.

Katz, A., Marks, D., McCarthy, G., and Spencer, S. (1991). Does interictal spiking change prior to seizures? Electroencephalog. Clin. Neurophysiol. *79*, 153–156.

Lange, H.H., Lieb, J., Jr., Engel, J., and Crandall, P. (1983). Temporospatial patterns of pre-ictal spike activity in human temporal lobe epilepsy. Electroencephalog. Clin. Neurophysiol. *56*, 543–555.

Le Van Quyen, M., Martinerie, J., Navarro, V., Boon, P., D'Havé, M., Adam, C., Renault, B., Varela, F., and Baulac, M. (2001). Anticipation of epileptic seizures from standard EEG recordings. The Lancet *357*, 183.

Lehnertz, K., and Elger, C. (1998). Can epileptic seizures be predicted? Evidence from nonlinear time series analysis of brain electrical activity. Phys. Rev. Lett. *80*, 5019–5022.

Liang, F., and Jones, E.G. (1997). Zif268 and Fos-like immunoreactivity in tetanus toxin-induced epilepsy: reciprocal changes in the epileptic focus and the surround. Brain Res. *778*, 281–292.

Lopes da Silva, F.H., Pijn, J.P., and Wadman, W.J. (1994). Dynamics of local neuronal networks: control parameters and state bifurcations in epileptogenesis. Prog. Brain Res. *102*, 359–370.

Lothman, E.W., and Williamson, J.M. (1994). Closely spaced recurrent hippocampal seizures elicit two types of heightened epileptogenesis: a rapidly developing, transient kindling and a slowly developing, enduring kindling. Brain Res. *649*, 71–84.

Martinerie, J., Adam, C., Quyen, M.L.V., Baulac, M., Clemenceau, S., Renault, B., and Varela, F. (1998). Epileptic seizures can be anticipated by non-linear analysis. Nat. Med. *4*, 1173–1176.

Noebels, J.L. (1999). Single-gene models of epilepsy. Adv. Neurol. *79*, 227–238.

Noebels, J.L., and Rutecki, P.A. (1990). Altered hippocampal network excitability in the hypernoradrenergic mutant mouse tottering. Brain Res. *524*, 225–230.

Noebels, J.L., Qiao, X., Bronson, R.T., Spencer, C., and Davisson, M.T. (1990). Stargazer: a new neurological mutant on chromosome 15 in the mouse with prolonged cortical seizures. Epilepsy Res. *7*, 129–135.

Osorio, I., Frei, M., and Wilkinson, S. (1998). Real-time automated detection and quantitative analysis of seizures and short-term prediction of clinical onset. Epilepsia *39*, 615–627.

Penfield, W., and Erickson, T.C. (1941). Epilepsy and cerebral localization (Springfield, IL: Charles C. Thomas).

Penfield, W., and Flanigin, H. (1950). Surgical therapy of temporal lobe seizures. Arch. Neurol. Psychiatr. *64*, 491–500.

Qin, D. (1995). A comparison of techniques for the prediction of epileptic seizures. In Eighth IEEE Symposium on Computer-Based Medical Systems (Lubbock, TX: IEEE Computer Society Press), pp. 151–157.

Qu, H., and Gotman, J. (1997). A patient-specific algorithm for the detection of seizure onset in long-term EEG monitoring: possible use as a warning device. IEEE Transactions of Biomedical Engineering *44*, 115–122.

Rajna, P., Clemens, B., Csibri, E., Dobos, E., Geregely, A., Gottschal, M., Gyo Horvath, A., Horvath, F, Mezofi, L., et al. (1997). Hungarian multicentre epidemiologic study of the warning and initial symptoms (prodrome, aura) of epileptic seizures. Seizure *6*, 361–368.

Ralston, B. (1958). The mechanism of transition of interictal spiking foci into ictal seizure discharge. Electroencephal. Clin. Neurophysiol. *10*, 217–232.

Risinger, M., Engel, J.J., VanNess, P., Henry, T., and Crandall, P.

(1989). Ictal localization of temporal seizures with scalp-sphenoidal recordings. Neurology *39*, 1288–1293.

Rogowski, Z., Gath, I., and Bental, E. (1981). On the prediction of epileptic seizures. Biol. Cybernet. *42*, 9–15.

Schiller, Y., Cascino, G., Busacker, N., and Sharbrough, F. (1998). Characterization and comparison of local onset and remote propagated electrographic seizures recorded with intracranial electrodes. Epilepsia *39*, 380–388.

Schuh, L.A., Henry, T.R., Ross, D.A., Smith, B.J., Elisevich, K., and Drury, I. (2000). Ictal spiking patterns recorded from temporal depth electrodes predict good outcome after anterior temporal lobectomy. Epilepsia *41*, 316–319.

Schwartzkroin, P.A., Baraban, S.C., and Hochman, D.W. (1998). Osmolarity, ionic flux, and changes in brain excitability. Epilepsy Res *32*, 275–285.

Spencer, S., Guimaraes, P., Katz, K., Kim, J., and Spencer, D. (1992). Morphological patterns of seizures recorded intracranially. Epilepsia *33*, 537–545.

Sperling, M. (1986). Electrophysiology of the ictal-interictal transition in humans. In Mechanisms of Epileptogenesis: The Transition to Seizure, M.A. Dichter, ed. (New York, NY: Plenum Press), pp. 17–38.

Sperling, M., and O'Connor, M. (1990). Auras and subclinical seizures: characteristics and prognostic significance. Ann. Neurol. *28*, 320–328.

Stein, A.G., Eder, H.G., Blum, D.E., Drachev, A., and Fisher, R.S. (2000). An automated drug delivery system for focal epilepsy. Epilepsy Res. *39*, 103–114.

Tang, C.M., Dichter, M., and Morad, M. (1990). Modulation of the N-methyl-D-aspartate channel by extracellular H+. Proc. Natl. Acad. Sci. USA *87*, 6445–6449.

Viglione, S., Ordon, V., and Risch, F. (1970). A methodology for detecting ongoing changes in the EEG prior to clinical seizures (West Huntington Beach, CA: McDonnel Douglas Astronautics Co.).

Wang, L., Nichols, T.C., Read, M.S., Bellinger, D.A., and Verma, I.M. (2000). Sustained expression of therapeutic level of factor IX in hemophilia B dogs by AAV-mediated gene therapy in liver. Mol. Ther. *1*, 154–158.

Ward, S., and Rise, M. (1998). Techniques for treating epilepsy by brain stimulation and drug infusion (US Patent #5713923).